Chemistry of Metals and Alloys

Chem. Met. Alloys 15 (2022) 26-33
Ivan Franko National University of Lviv
www.chemetal-journal.org

Electrochemical hydrogenation properties of Nd_2MgT_9 (T = 3*d*-metals) multi-phase alloys

Yuriy VERBOVYTSKYY[1], Volodymyr OPRYSK[1], Yuriy DUBOV[1], Ihor ZAVALIY[1]*

[1] *Karpenko Physico-Mechanical Institute, NAS of Ukraine, Naukova St. 5, 79060 Lviv, Ukraine*
** Corresponding author. E-mail: ihor.zavaliy@gmail.com*

Received May 3, 2022; accepted June 29, 2022; available on-line September 1, 2022
https://doi.org/10.30970/cma15.0426

A series of alloys based on the intermetallic compounds Nd_2MgNi_9 and Nd_2MgCo_9 with the compositions Nd_2MgT_8T' (T = Ni, Co, T' = Fe, Co, Ni, Cu) and $Nd_2MgNi_{9-x}Co_x$ (x = 0, 3, 4.5, 6, 9) were synthesized and their electrochemical hydrogenation properties studied. The alloys contained three phases: pseudo-binary AB_2 Laves ($SnMgCu_4$ structure type), AB_3 ($PuNi_3$ structure type), and AB_5 ($CaCu_5$ structure type) phases. Electrochemical characteristics such as discharge capacity and capacity retention were studied. The highest capacity (297 mA h/g) was achieved by the $Nd_2MgNi_{9-x}Co_x$ (x = 6) alloy and may be related to the chemical and multi-phase composition.

X-ray powder diffraction / AB_3 alloys / Transition metals / Electrochemical hydrogenation

1. Introduction

Ni-MH batteries are important representatives of portable power sources, because of their high capacity, simple storage and transportation, environmentally friendly composition, and recyclability. Still, the search for increasing energy density continues for this type of batteries. Many different classes of intermetallic compounds may be used as materials for negative electrodes, for instance, AB_2, AB_3, A_2B_7, and A_5B_{19} (based on rare-earth and transition metals) [1-3]. Special attention is dedicated to AB_3 alloys, as one of the important and novel classes of intermetallic hydrides [4]. Among the different alloy systems, *R*-Mg-Ni-based hydrogen storage alloys have become a research focus because of the advantages of their high discharge capacity and good activation properties. It has also been shown that partial replacement of the rare-earth metal by magnesium has a positive impact on the discharge capacity for this type of alloy [5-9]. $La_{3-x}Mg_xNi_9$ (x = 1; 1.1; 1.2) alloys showed maximum discharge capacities in the range of up to 370-399 mA h/g (at 100 mA/g current density), depending on the Mg content, losing up to 45% of the capacity after 200 charge/discharge cycles [10]. Doping of AB_3 alloys, besides improving the capacity, also has a positive impact on cycling stability of the electrode material [11]. Alloys with replacement of La by another rare-earth metal (*e.g.* Nd) appear to be superior, as compared to the La_2MgNi_9 counterpart, with respect to the delivered discharge capacity. The introduction of Nd further leads to a flatter and longer discharge plateau [12]. Many efforts have been made to improve the electrochemical properties of such alloys by different element substitutions, annealing treatments, and surface modifications. This work is a continuation of our systematic studies on hydrogen-storage alloys. We here present an investigation of the phase analysis, structure refinement, and electrochemical hydrogenation of alloys based on the intermetallic compounds Nd_2MgNi_9 and Nd_2MgCo_9 with transition metal substitution: $Nd_2MgNi_{9-x}Co_x$ (x = 0, 3, 4.5, 6, 9) and Nd_2MgT_8T' (T, T' = Fe, Co, Ni, Cu).

2. Experimental details

The alloys were prepared by the sintering method. Nd_2M_9 precursors (M = Ni, Co, Fe, Cu; purity ≥ 99.9%) and Mg powder (Alfa Aesar, 325 mesh, 99.8%) were used as starting materials. The precursors were synthesized by arc melting from pure metals in a purified argon atmosphere. The ingots were crushed and mixed with Mg powder in stoichiometric proportions with addition of 3 wt.% excess of Mg to compensate for possible deviations from the nominal composition due to Mg evaporation during sintering. The mixtures were pressed into pellets at 10 ton/cm^2. The total weight of each sample was in the range 2-3 g. The pellets were placed into stainless steel crucibles and sealed under argon. The samples were heated up to 800°C and cooled to 500°C over one week and annealed at 500°C for three weeks.

Structural analysis of the samples was carried out by X-ray powder diffraction (XRD) using a DRON-3M diffractometer (Cu-*Kα* radiation). Phase analysis and crystal structure refinement were conducted with the help of the PowderCell [13] and FullProf [14] software package.

Electrode materials made of the alloys were prepared by mixing with carbonyl Ni powder in the ratio 1:3 (wt.). Pellet electrodes with a diameter of 12 mm were made by cold-pressing the powder mixture under a pressure of 10 ton/cm^2 and then sandwiched between two Ni foams with the fixed conductor. The electrochemical properties were tested in a three-electrode system. Platinum auxiliary and metal hydride (MH) working electrodes were placed in a glass cell filled with a 6M KOH solution, while an Ag/AgCl reference electrode was connected to the system via an agar bridge. The electrochemical charge/discharge properties of the synthesized alloys were measured at a current density of 50 mA/g and a potential ranging from −0.6 V to −1.2 V versus the Ag/AgCl electrode. All electrochemical measurements were performed at room temperature.

3. Results and discussion

3.1. Phase analysis

A series of samples based on the intermetallic compounds Nd_2MgNi_9 and Nd_2MgCo_9 were prepared and characterized. According to the analysis by X-ray diffraction the Nd_2MgNi_9 alloy was multi-phase, and its crystallographic data were in good agreement with literature data [15,16], while the Nd_2MgCo_9 alloy contained mostly the AB_3 phase (> 90 wt.%) with $PuNi_3$ structure type (its crystallographic data were described in [17]). For the Nd_2MgT_8T' (T = Ni, Co, T' = Fe, Co, Ni, Cu) samples, three phases were detected: pseudo-binary AB_2 Laves phase ($SnMgCu_4$ structure type) + AB_3 ($PuNi_3$ structure type) + AB_5 ($CaCu_5$ structure type). For the substituted Ni-alloys (Nd_2MgNi_8T', T' = Fe, Co, Cu), the majority phase was the pseudo-binary $NdMg(Ni,T')_4$ compounds, while in the case of the Co-based alloys, the highest content was observed for the AB_3 phase. Results of the XRD phase analysis on the compositions of the Nd_2MgT_8T' alloys are provided in Table 1. It can be seen that addition of Fe and Cu decreases the formation of the AB_3 phase. Refined XRD patterns of selected alloys are presented in Fig. 1.

Similar trends were observed for the alloys with gradual substitution of Co for Ni in the $Nd_2MgNi_{9-x}Co_x$ (x = 0, 3, 4.5, 6, and 9) alloys. Co substitution for Ni in Nd_2MgNi_9 promotes the formation of a multi-phase alloy with a relatively high content of AB_3 phase. A mixture of the $Nd_2Mg(Ni,Co)_9$, $NdMg(Ni,Co)_4$ and $Nd(Ni,Co)_5$ intermetallic compounds was detected in the $Nd_2MgNi_{9-x}Co_x$ samples with x = 3, 4.5, and 6. More detailed results of the XRD analysis and structure refinements, and XRD patterns for the $Nd_2MgNi_{9-x}Co_x$ alloys, are presented in Table 2 and in Fig. 2.

Table 1 Results of the XRD phase analysis and structure refinement for the Nd_2MgT_8T' alloys (T = Ni, Co, T' = Fe, Co, Ni, Cu).

Alloy composition	Phases	*a*, Å	*b*, Å	*c*, Å	*γ*, °	Phase content, wt.%
Nd_2MgNi_8Fe	$NdMg(Ni,Fe)_4$	7.0973(7)	7.0973(7)	7.0973(7)	90	65
	$Nd(Ni,Fe)_5$	4.9884(9)	4.9884(9)	3.999(1)	120	29
	$Nd_2Mg(Ni,Fe)_9$	4.992(3)	4.992(3)	24.05(1)	120	6
Nd_2MgNi_8Co	$NdMg(Ni,Co)_4$	7.0870(6)	7.0870(6)	7.0870(6)	90	56
	$Nd(Ni,Co)_5$	4.9687(9)	4.9687(9)	3.975(1)	120	30
	$Nd_2Mg(Ni,Co)_9$	4.9709(9)	4.9709(9)	24.082(8)	120	14
Nd_2MgNi_8Cu	$NdMg(Ni,Cu)_4$	7.0951(6)	7.0951(6)	7.0951(6)	90	65
	$Nd(Ni,Cu)_5$	4.9771(9)	4.9771(9)	3.985(1)	120	23
	$Nd_2Mg(Ni,Cu)_9$	4.9772(9)	4.9772(9)	24.101(5)	120	12
Nd_2MgCo_8Fe	$Nd(Co,Fe)_5$	4.986(4)	4.986(4)	4.001(6)	120	73
	$NdMg(Co,Fe)_4$	7.078(6)	7.078(6)	7.078(6)	90	24
	$Nd_2Mg(Co,Fe)_9$	4.88(1)	4.88(1)	23.6(2)	120	3
Nd_2MgCo_8Ni	$Nd_2Mg(Co,Ni)_9$	5.024(2)	5.024(2)	24.18(1)	120	81
	$NdMg(Co,Ni)_4$	7.112(5)	7.112(5)	7.112(5)	90	10
	$Nd(Ni,Co)_5$	4.961(3)	4.961(3)	3.83(3)	120	9
Nd_2MgCo_8Cu	$Nd_2Mg(Co,Ni)_9$	5.043(3)	5.043(3)	24.23(2)	120	63
	$Nd(Ni,Co)_5$	5.037(5)	5.037(5)	4.05(1)	120	24
	$NdMg(Co,Ni)_4$	7.173(7)	7.173(7)	7.173(7)	90	13

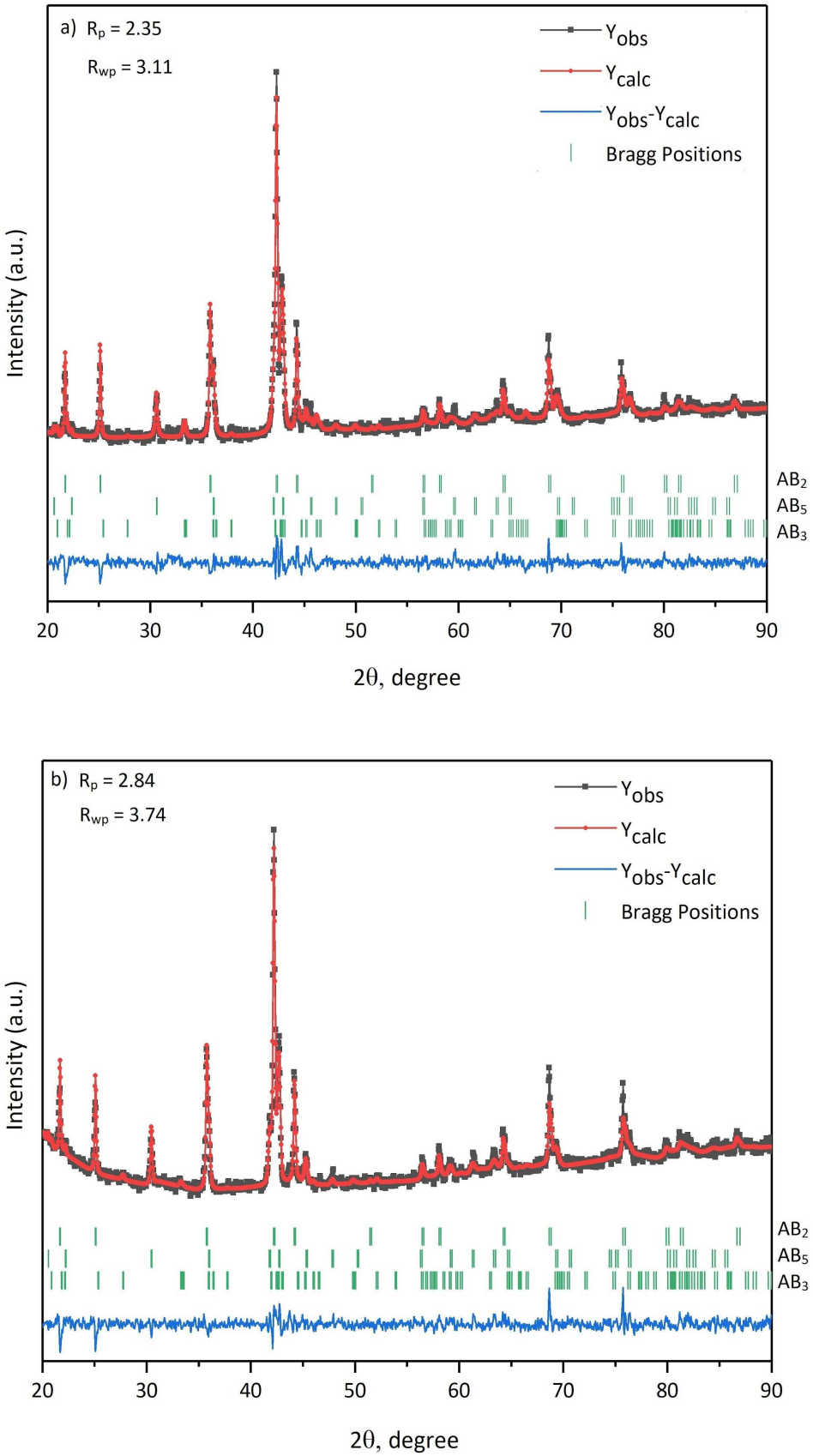

Fig. 1 Refined XRD patterns for a) Nd_2MgNi_8Co; b) Nd_2MgNi_8Fe.

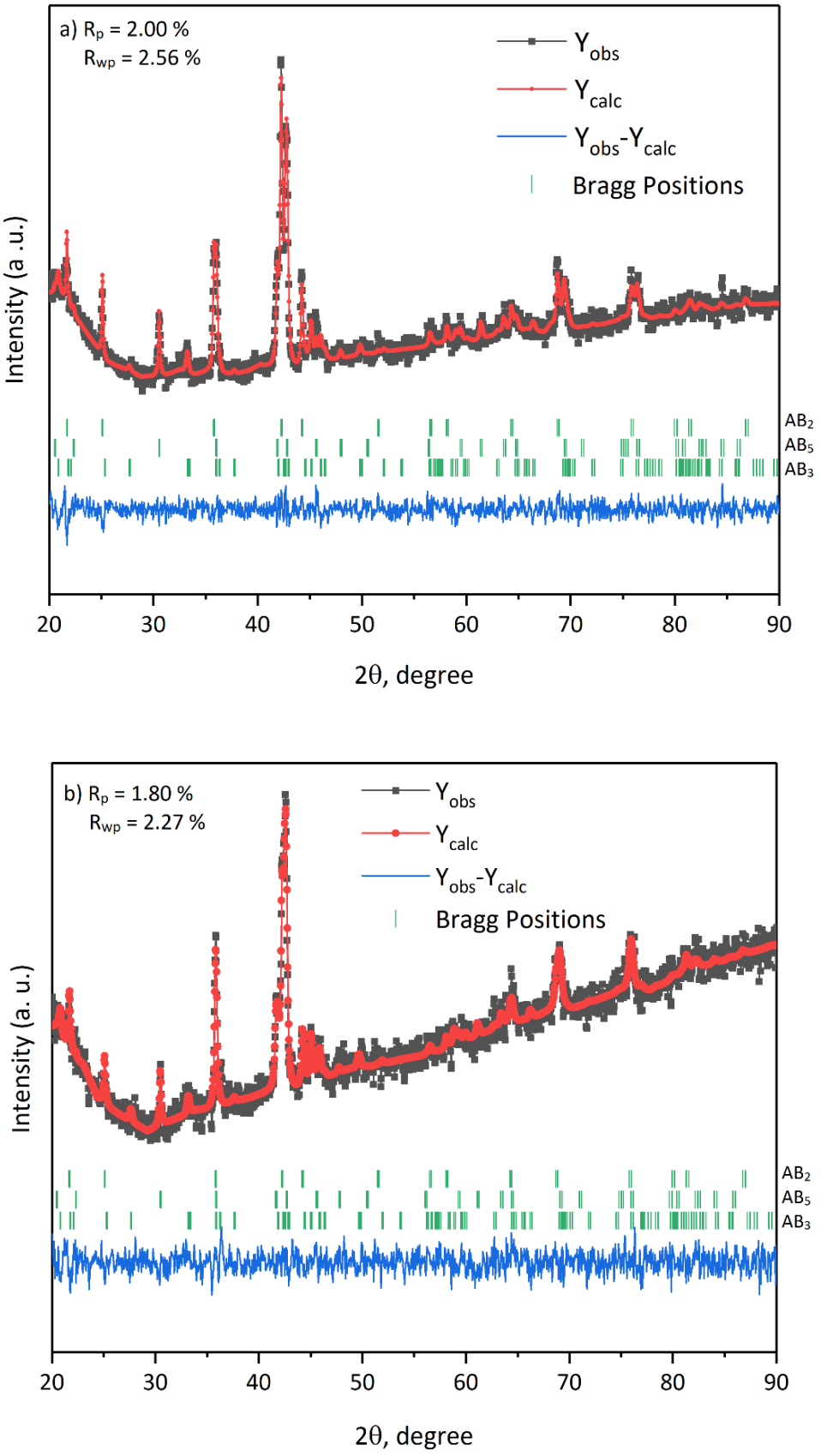

Fig. 2 Refined XRD patterns for a) $Nd_2MgNi_6Co_3$; b) $Nd_2MgNi_3Co_6$.

Table 2 Results of XRD phase analysis and structure refinements for $Nd_2MgNi_{9-x}Co_x$ (x = 0, 3, 4.5, 6, and 9).

Alloy composition	Phases	*a*, Å	*b*, Å	*c*, Å	*γ*, °	Phase content, wt.%
Nd_2MgNi_9	$NdMgNi_4$	7.084(3)	7.084(3)	7.084(3)	90	22
	$Nd_{1.5}Mg_{0.5}Ni_7$	5.011(3)	5.011(3)	24.744(7)	120	20
	Nd_2MgNi_9	5.0255(6)	5.0255(6)	24.700(6)	120	58
$Nd_2MgNi_6Co_3$	$NdMg(Ni,Co)_4$	7.092(1)	7.092(1)	7.092(1)	90	35
	$Nd(Ni,Co)_5$	4.984(1)	4.984(1)	3.976(2)	120	22
	$Nd_2Mg(Ni,Co)_9$	4.988(1)	4.988(1)	24.103(9)	120	43
$Nd_2MgNi_{4.5}Co_{4.5}$	$NdMg(Ni,Co)_4$	7.095(1)	7.095(1)	7.095(1)	90	25
	$Nd(Ni,Co)_5$	4.997(2)	4.997(5)	3.979(2)	120	19
	$Nd_2Mg(Ni,Co)_9$	4.997(2)	4.997 (2)	24.098(1)	120	56
$Nd_2MgNi_3Co_6$	$NdMg(Ni,Co)_4$	7.094(2)	7.094(2)	7.094(2)	90	26
	$Nd(Ni,Co)_5$	5.006(2)	5.006(2)	3.977(2)	120	16
	$Nd_2Mg(Ni,Co)_9$	5.007(2)	5.007(2)	24.124(1)	120	58
Nd_2MgCo_9 [a]	Nd_2MgCo_9	5.0362(2)	5.0362(2)	24.189(1)	120	95
	$NdCo_5$	5.034(1)	5.034(1)	3.973(1)	120	5

[a] data from [17]

Table 3 Electrochemical characteristics of the Nd_2MgT_8T' (T = Ni, Co, T' = Fe, Co, Ni, Cu) alloys.

Electrode	C_{max}, mAh/g	C_N, mAh/g	S_N, %	N (cycle)
Nd_2MgNi_8Co	211	182	86	50
Nd_2MgNi_8Fe	212	159	75	50
Nd_2MgNi_8Cu	172	153	89	50
Nd_2MgCo_8Ni	185	116	62	50
Nd_2MgCo_8Fe	112	112	100	50
Nd_2MgCo_8Cu	77	55	72	50

3.2. Electrochemical hydrogenation

All the prepared samples were subjected to electrochemical hydrogenation. The samples with high Ni content showed better electrochemical properties. Detailed results of the electrochemical measurements are provided below.

The electrochemical investigations of the Nd_2MgNi_9 and Nd_2MgCo_9 electrodes revealed low discharge capacity, 172 mAh/g and 67 mAh/g, respectively. The effect of the transition metal substitution in the Nd_2MgT_8T' (T = Ni, Co; T' = Fe, Co, Ni, Cu) alloys on the electrochemical properties was also investigated. Data for the discharge capacity and its change with cycling is provided in Table 3. Electrochemical measurements showed that their maximum discharge capacity does not exceed ~212 mAh/g (Nd_2MgNi_8Co and Nd_2MgNi_8Fe) at a charge/discharge current density of 50 mA/g. The best cycling stability, 89%, was found for the Nd_2MgNi_8Cu alloy. These results are presented in Fig. 3. The worst cycling stability for this series of alloys was observed for Nd_2MgCo_8Ni, which loses more than 36% of its maximum capacity. The Nd_2MgCo_8Fe sample demonstrated an increase of the discharge capacity for all of the 50 charge-discharge cycles, not having reached the maximum and not having passed the activation. In general. The Ni-based alloys (Nd_2MgNi_8T (T = Fe, Co, Cu)) exhibited better electrochemical characteristics (Fig. 3*a*) than the Co-based ones. The addition of Ni also had a remarkable impact on the Nd_2MgCo_8T alloy (Fig. 3*b*), where the best capacity was observed for the Ni-substituted sample, but with a high decrease of the capacity during cycling.

Results of the electrochemical hydrogenation of the $Nd_2MgNi_{9-x}Co_x$ (x = 0, 3, 4.5, 6, 9) alloys presented in Fig. 4. The samples with x = 3, 4.5, 6 required up to 3 activation cycles to achieve their maximum discharge capacity. The alloys with only Ni or Co needed up to 6-7 activation cycles. The mixtures of $Nd_2Mg(Ni,Co)_9$, $NdMg(Ni,Co)_4$ and $Nd(Ni,Co)_5$ intermetallic compounds detected in the $Nd_2MgNi_{9-x}Co_x$ samples with x = 3, 4.5 and 6, however, showed notably greater capacity: 248 mAh/g (x = 3), 289 mAh/g (x = 4.5) and 297 mAh/g (x = 6), respectively. The discharge capacity retention over 50 cycles at charge/discharge current density of 50 mA/g was remarkably heightened from 68% (x = 6) to 76% (x = 3), respectively. Discharge capacity and cycling stability for the $Nd_2MgNi_{9-x}Co_x$ (x = 0, 3, 4.5, 6, 9) alloys is presented in Table 4. As we can see, the alloys with low Co content showed better discharge capacity retention.

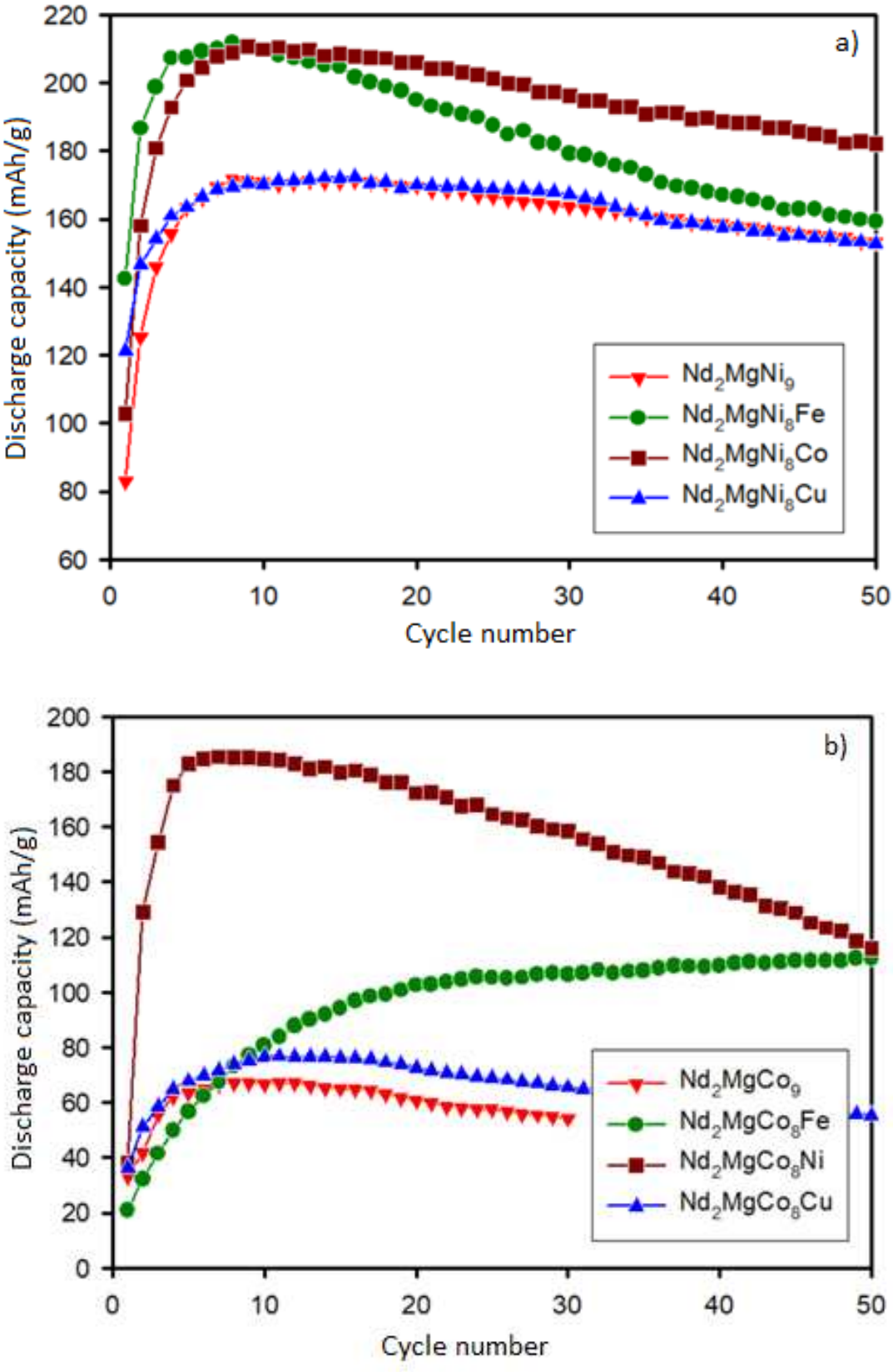

Fig. 3 Discharge capacity *vs* cycle number for: a) Nd_2MgNi_8T (T = Fe, Co, Cu); b) Nd_2MgCo_8T (T = Fe, Ni, Cu), current density 50 mA/g.

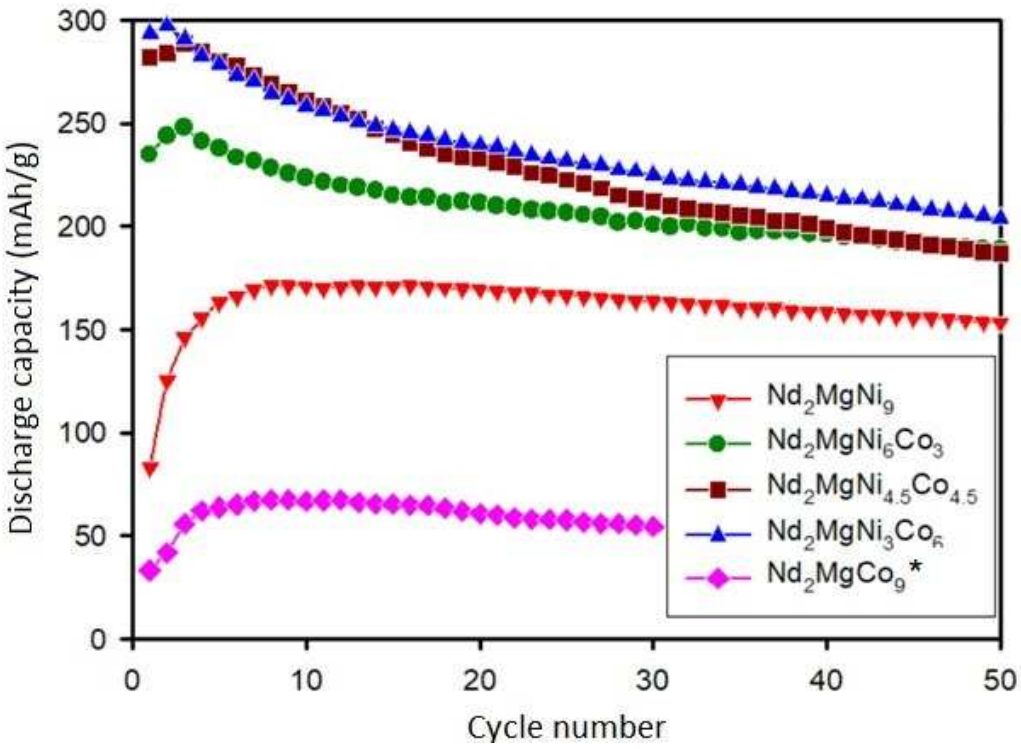

Fig. 4 Discharge capacity *vs* cycle number for $Nd_2MgNi_{9-x}Co_x$ (x = 0, 3, 4.5, 6, 9), current density 50 mA/g (data for x = 0 from [17]).

Table 4 Electrochemical characteristics of the $Nd_2MgNi_{9-x}Co_x$ (x = 0, 3, 4.5, 6, 9) alloys.

Electrode	C_{max}, mAh/g	C_N, mAh/g	S_N, %	N (cycle)
Nd_2MgNi_9	172	153	89	50
$Nd_2MgNi_6Co_3$	248	189	76	50
$Nd_2MgNi_{4.5}Co_{4.5}$	289	188	65	50
$Nd_2MgNi_3Co_6$	297	204	69	50
Nd_2MgCo_9 [a]	67	54	85	30

[a] data from [17]

Conclusions

All the $Nd_2Mg(T,T')_9$ alloys prepared here were found to contain three phases (pseudo-binary AB_2, AB_3, and AB_5). The following trend was observed for the Nd_2MgT_8T'alloys: the Ni-based alloys were characterized by a high content of the pseudo-binary AB_2 phase, while the Co-based alloys contained more of the AB_3 phase. Increasing the Co content For the $Nd_2MgNi_{9-x}Co_x$ (x = 0, 3, 4.5, 6, 9), produced an increase of the AB_3 content.

The $Nd_2MgNi_{9-x}Co_x$ (x = 0, 3, 4.5, 6, 9) alloys showed notably greater capacity for the higher Co contents: 248 mAh/g (x = 3), 289 mAh/g (x = 4.5) and 297 mAh/g (x = 6), respectively. Such a high discharge capacity may be a result of the synergetic effect of the multiple phase composition of the alloys. The discharge capacity retention over 50 cycles at a charge/discharge current density of 50 mA/g decreased from 76% (x = 3) to 69% (x = 6).

The effect of the transition metal substitution in the Nd_2MgT_8T' (T = Ni, Co; T' = Fe, Co, Ni, Cu) alloys on the electrochemical properties were also investigated. The maximum discharge capacity did not exceed ~210 mAh/g (Nd_2MgNi_8Co and Nd_2MgNi_8Fe) at a charge/discharge current density of 50 mA/g. The best cycling stability of 89% was found for the Nd_2MgNi_8Cu alloy.

References

[1] H. Yan, W. Xiong, L. Wang, B. Li, J. Li., X. Zhao, *Int. J. Hydrogen Energy* 42 (2017) 2257-2264. *https://doi.org/10.1016/j.ijhydene.2016.09.049*

[2] Yu.V. Verbovyts'kyi, I.Yu. Zavalii, *Mater. Sci.* 51 (2016) 443-456. *https://doi.org/10.1007/s11003-016-9861-0*

[3] Yu.V. Verbovyts'kyi, I.Yu. Zavalii, *Mater. Sci.* 52

(2017) 747-759.
https://doi.org/10.1007/s11003-017-0018-6

[4] W. Liu, C.J. Webb, E.MacA Gray, *Int. J. Hydrogen Energy* 41 (2016) 3485-3507.
https://doi.org/10.1016/j.ijhydene.2015.12.054

[5] E. Akiba, H. Hayakawa, T. Kohno, *J. Alloys Compd*. 408-412 (2006) 280-283.
https://doi.org/10.1016/j.jallcom.2005.04.180

[6] R.V. Denys, V.A. Yartys, *J. Alloys Compd.* 509 (2011) S540-S548.
https://doi.org/10.1016/j.jallcom.2010.11.205

[7] L. Zhang, J. Wang, W. Du, Y. Ding, Y. Li, S. Yang, S. Han, Y. Fan, *J. Alloys Compd.* 653 (2015) 498-505.
https://doi.org/10.1016/j.jallcom.2015.09.049

[8] B. Liao, Y.Q. Lei, G.L. Lu, L.X. Chen, H.G. Pan, Q.D. Wang, *J. Alloys Compd.* 356-357 (2003) 746-749.
https://doi.org/10.1016/s0925-8388(03)00083-5

[9] V. Shtender, V. Paul-Boncour, R. Denys, D. Hedlund, P. Svedlindh, I. Zavaliy, *Mater. Res. Bull.* 156 (2022) 111981.
https://doi.org/10.1016/j.materresbull.2022.111981

[10] C. Wan, W. Hu, R.V. Denys, C.C. Nwakwuo, J.K. Solberg, V.A. Yartys, *J. Alloys Compd.* 856 (2021) 157443.
https://doi.org/10.1016/j.jallcom.2020.157443

[11] Y. Liu, Y. Cao, L. Huang, M. Gao, H. Pan, *J. Alloys Compd.* 509 (2011) 675-686.
https://doi.org/10.1016/j.jallcom.2010.08.157

[12] A.A. Volodin, C. Wan, R.V. Denys, G.A. Tsirlina, B.P. Tarasov, M. Fichtner, U. Ulmer, Y. Yu, C.C. Nwakwuo, V.A. Yartys, *Int. J. Hydrogen Energy* 41 (2016) 9954-9967.
https://doi.org/10.1016/j.ijhydene.2016.01.089

[13] W. Kraus, G. Nolze, *PowderCell for Windows* (version 2.4), Berlin: Federal Institute for Materials Research and Testing, 1999.

[14] J. Rodriguez-Carvajal, T. Roisnel, *FullProf.98 and WinPLOTR: New Windows 95/NT Applications for Diffraction Commission For Powder Diffraction*, International Union for Crystallography, Newsletter No.20 (May-August) Summer, 1998.

[15] V. Yartys, R. Denys, *J. Alloys Compd.* 645 (2015) S412-S418.
https://doi.org/10.1016/j.jallcom.2014.12.091

[16] V. Yartys, R. Denys, *Chem. Met. Alloys* 7 (2014) 1-8.
https://doi.org/10.30970/cma7.0243

[17] V.V. Shtender, R.V. Denys, V. Paul-Boncour, I.Yu. Zavaliy, Yu.V. Verbovytskyy, D.D. Taylor, *J. Alloys Compd.* 695 (2017) 1426-1435.
https://doi.org/10.1016/j.jallcom.2016.10.268